First-principles study of quantum size effects in ultrathin Pb-Bi metal alloy films

Yu Jia,[1,2] S. Y. Wang,[3] W. G. Chen,[1] Q. Sun,[1] H. H. Weitering,[4,2] and Zhenyu Zhang[2,4,5]
[1]*School of Physics and Engineering, Zhengzhou University, Zhengzhou, Henan 450052, China*
[2]*Materials Science and Technology Division, Oak Ridge National Laboratory, Oak Ridge, Tennessee 37831, USA*
[3]*Department of Optical Science and Engineering and Key Laboratory of Advanced Photonic Materials and Devices, Fudan University, Shanghai 200433, China*
[4]*Department of Physics and Astronomy, The University of Tennessee, Knoxville, Tennessee 37996, USA*
[5]*ICQD, University of Science and Technology of China, Hefei, Anhui 230026, China*
(Received 4 January 2010; revised manuscript received 7 May 2010; published 21 June 2010)

Using first-principles calculations within density-functional theory (DFT), we investigate the effect of Bi doping in ultrathin Pb(111) films on tuning the quantum size effects (QSEs) of random metal alloy films. Our results show that the QSE of Pb films, as manifested by the oscillatory surface energy, work function, interlayer spacing, and stability with film thickness, are robust against the introduction of random scattering centers doped in the films. Specifically, the stability and the work function of the ultrathin random-alloy films exhibit obvious quantum oscillations up to ~20% Bi doping. The periodicity of the beating pattern of QSE oscillations can be tuned via the concentration of the doped Bi atoms through changing the Fermi wave vector. For $Pb_{0.89}Bi_{0.11}$ alloy films, the role of the substrates of Si(111) and Ge(111) is also studied and the results are consistent with our recent experimental studies.

DOI: 10.1103/PhysRevB.81.245425 PACS number(s): 68.55.−a, 73.21.Fg, 71.15.Nc

I. INTRODUCTION

In both nanoscience and nanotechnology, one of the key issues in achieving desired functionalities within quantum engineering is to control the material size at the nanoscale. The phrase "quantum engineering" generally refers to the possibility of creating novel electronic structures through atomic-scale control of quantum-mechanical boundary conditions, and recent experimental developments in the epitaxial growth of metallic thin films have offered such a possibility. It has been found that some metals can form atomically "flat" continuous films or large islands with atomically flat tops with selective heights.[1–4] More importantly, it has been found that the properties of these films such as the work function,[3] thermal expansion,[4] chemical reactivity,[5,6] superconducting transition temperature T_c,[7,8] and electron-phonon coupling[9,10] can all strongly depend on the film thickness. This indicates that the properties of the films can be adjusted by controlling the film thickness at the atomic scale and such epitaxial systems include Ag/GaAs(110),[2] Ag/Si(111),[11] Ag/Fe(100),[12] Pb/Si(111),[13–23] Pb/Cu(111),[24] Pb/Ge(100),[25] and Pb/Ge(111).[26] This interesting phenomenon is commonly attributed to the quantum size effects (QSEs).[27–30] Due to the small dimension perpendicular to the metallic films and the confinement of the interfaces, the electronic energy bands are discretized and form quantum-well states (QWSs) along the vertical direction.[31–39] The QWS can lead to the oscillatory dependence of the film total energy on its thickness, instead of the linear dependence on thickness for very thick films. This oscillatory behavior implies that a thin film with a certain number of layers may be energetically favorable and hence become atomically flat. In comparison with other films, the Pb(111) films exhibit one striking feature: the QSE is very robust as the preferred thickness can be over 30 monolayers (MLs).[39] The reason for this uniqueness is that Pb's Fermi wavelength, λ_F, is almost perfectly commensurate with the interlayer spacing d along the [111] direction, given by $2.07d \approx 3\lambda_F/2$. The accidental matching of the electronic and crystallographic length scales results in re-entrant bilayer-by-bilayer (RBBB) growth under appropriate kinetic growth conditions. The RBBB growth mode represents a novel quantum growth phenomenon that is characterized by a strong preference for bilayer growth with periodic interruptions of a monolayer (or even a trilayer[30]). The periodic interruption of the bilayer growth follows a well-defined beating pattern with a superperiod of 9 ML, which is due to the fact that λ_F and d are not exactly commensurate. This suggests the possibility of altering the quantum growth mode by tuning the Fermi wave vector k_F through doping different amount of other metals, which can extend the concept of electronic growth to multicomponent nanostructures.

In this paper, we have carried out density-functional theory (DFT) calculations of the QSE of PbBi alloy films up to 40 ML. Considering that the atomic radii of the doping elements should be close to that of Pb (to minimize local strain effects), we choose Bi as the doping element in our studies. Each Bi atom has five outmost electrons as conduction electrons, one more than that of a Pb atom. We therefore call this kind of dopant in Pb "*n-like dopant*," just like the *n* doping in semiconductors. Our calculations have shown that the QSE of the PbBi alloy films is robust against Bi doping up to 20% and the spatial distribution of the dopants only have a marginal effect. Moreover, we find the periodicity of the beating pattern of the QSE oscillation can be tuned by the Bi doping level, which can be fully explained by the change in the Fermi wave vector k_F. Finally, the effects of substrate are considered and the calculated results agree near perfectly with our recent experiments.

The paper is organized as follows. In Sec. II we briefly describe our calculation methods. In Sec. III we present the calculated results of $Pb_{1-x}Bi_x(111)$ (x=6%, 11%, and 14%, respectively) alloy films. Surface energy and stability of the

alloy films are discussed with respect to the thickness. In Sec. IV the influence of the substrate Si(111) and Ge(111) is studied. In Sec. V, we show that, when the Bi concentration is low, a simple free-electron model can already capture the essence of the QSE in PbBi alloy films and explain most of the DFT results, especially the change in the beating pattern period of QSE oscillations. Discussions and conclusions are summarized in Sec. VI.

II. CALCULATION METHODS

A. General description

Our calculations are based on DFT. The Vienna *ab initio* simulation package (VASP) is used to solve the Kohn-Sham equations with periodic boundary conditions and a plane-wave basis set.[40–44] We use the Perdew-Wang version[45] of the generalized gradient approximation (GGA) to treat the electron exchange and correlation functional. In our calculations, the 6*s* and 6*p* electrons of the Pb and Bi atoms are treated as valence electrons and the 5*d* electrons treated as core ones. For the Si(Ge) atom, the valence electrons are chosen to be the $3s(4s)$ and $3p(4p)$. Default plane-wave cutoffs (144 eV) from the GGA ultrasoft pseudopotentials are used in our calculations.[46] The Monkhorst-Pack scheme[47] is adopted for the Brillouin-zone (BZ) sampling. To accelerate the electronic relaxation, we apply the Fermi-level smearing approach of Methfessel and Paxton[48] with proper parameters. With the above setting, the lattice constants for bulk Pb, Si, and Ge are calculated to be 0.504 nm, 0.543 nm, and 0.576 nm, respectively. These values are larger than the experimental values for Pb, Si, and Ge by 1.8%, 4%, and 1.7%, respectively. In all the calculations, the spin-orbit coupling is neglected.[39] In our slab model, the vacuum layer between neighboring periodic slabs is fixed at 12 ML, which is large enough to ensure the decoupling of repeated slabs.

B. Specifics for different doping levels and substrates

For alloy films with dilute dopants, the supercells should be very large in order to describe the random distribution of the dopants, resulting in several hundred atoms in each unit cell. It is impossible to perform such *ab initio* calculations due to the limitation of computing power. So to study the QSE of alloy films we use smaller supercells with proper distributions of dopants in different layers of the alloy films. In the calculations of freestanding $Pb_{1-x}Bi_x$ alloy films, we use different kinds of supercells to simulate the different alloy compositions. We use 4×4, 3×3, and $\sqrt{7}\times\sqrt{7}$ unit cells along the [111] direction of Pb and replace one Pb atom by a Bi atom in each layer so that they correspond to 6%, 11.3% and 14% Bi doping, respectively.

The Brillouin-zone sampling is done with $5\times5\times1$ *k*-point meshes and the results are cross checked by using $7\times7\times1$ *k*-point meshes for the 3×3 supercells, i.e., the $Pb_{0.89}Bi_{0.11}$ alloy film. We use $6\times6\times1$ and $9\times9\times1$ *k*-point meshes for the 4×4 and $\sqrt{7}\times\sqrt{7}$ supercells, respectively. All the atoms in the supercells are fully relaxed until all the forces on the relaxed atoms are less than 0.03 eV/Å.

We also study the influence of the Si(111) and Ge(111) substrates on the $Pb_{0.89}Bi_{0.11}(111)$ alloy film. Since the mismatch of the lattice constants between the PbBi alloy and the substrate is about 8% for Si and 11% for Ge, it impossible to carry out direct first-principles calculations for these epitaxial systems. Similar to our previous efforts[30] to overcome this problem, we use a Si(111)-$\sqrt{7}\times\sqrt{7}$ surface unit cell to match the $Pb_{1-x}Bi_x(111)$ (3×3) film by rotating the substrate by 19.1°, resulting in a perfect lattice match at the interface. Although this rotation is rather artificial, the Si or Ge substrates still retain their semiconducting properties because we have only compressed the substrate to reach lattice match.[19] To be more specific, the $Pb_{1-x}Bi_x$/Si(Ge)(111) system is modeled by a series of 3×3 PbBi supercells on a ten-layer Si(Ge)(111)-$\sqrt{7}\times\sqrt{7}$-*R*19.1° substrate. For the Si(Ge)(111) layers, the six layers of Si(Ge) atoms near the $Pb_{1-x}Bi_x$/Si(Ge)(111) interface are allowed to relax and the remaining four layers at the bottom are fixed at their respective bulk positions. The Brillouin-zone sampling is done with a $3\times3\times1$ *k*-point mesh and the energy convergence is reached when all the forces on the relaxed atoms are less than 0.05 eV/Å.

C. Surface energy and the stability of alloy films

We first calculate the total energies of films of different thickness. This total energy can be viewed as the energy of the bulk alloy with the same thickness and the small deviation from this energy caused by the two film interfaces. As a result, these total energies should increase linearly with the film thickness modulated by some small fluctuations. We then fit the data with a linear function and after subtracting the linear part from the total energies, we are left with the small fluctuations of the total energies, which are the desired surface energies.[49–51]

For an alloy film of *N* layers, the total energy of the film with two opposite surfaces is labeled as $E_{total}(N)$. Then the surface energy E_s of the film can be written as

$$E_s = 1/2(E_{total} - NE_{bulk}). \tag{1}$$

In order to discuss the stability of the film, we define a quantity, the second difference of E_s, *by*

$$\Delta^2 E(N) = E_s(N+1) + E_s(N-1) - 2E_s(N). \tag{2}$$

If $\Delta^2 E(N) \geq 0$, the film of *N* MLs is stable, otherwise the film is unstable.[29,30] As a film grows thicker, its properties approach those of its bulk. In other words, for a thick film, its properties should change little with the addition or removal of 1 ML. Therefore, we expect that for large *N* the second difference $\Delta^2 E(N)$ is very small, $|\Delta^2 E(N)| \ll 1$. Reversely, when $|\Delta^2 E(N)| \ll 1$ for a given layer number, we say that the film of *N* MLs is bulk like. Then the films will grow layer by layer.

III. TUNING THE QUANTUM STABILITY OF ULTRATHIN METAL ALLOY FILMS

A. Lattice constants of the alloy films

Before we begin to study the stability of the alloy films, we first calculate the lattice constants of alloy films with

TABLE I. Lattice constants (a) of $Pb_{1-x}Bi_x$ alloys at different Bi concentrations (x) from our DFT calculations. The lattice constant units are in Å.

	$Pb_{1-x}Bi_x$				
x	0.00	0.06	0.11	0.14	0.25
a	5.040	5.048	5.056	5.060	5.063

different doping concentration. Two methods are adopted to calculate the lattice constants for a given doping concentration. One is that we choose a different $m \times n \times l$ unit cell as the bulk case, such as $3\times3\times3$, $3\times3\times2$, $2\times2\times4$, $2\times2\times3$, $2\times2\times2$, and $2\times2\times1$. In each unit cell, one Pb atom is replaced by one Bi atom and therefore the doping concentration corresponds to 3.7%, 5.5%, 6.2%, 8.3%, 12.5%, and 25%, respectively. The lattice constants of the alloys are determined by minimizing the total energy of the supercells. From these calculated results, we can obtain the lattice constant for a given doping content by using the interpolation method. Another method to calculate the lattice constants is that we can utilize an $m\times m\times3$ supercell. This supercell corresponds to three layers in the [111] direction and an $m\times m$ cell in the [110] and [101] directions because of the three-layer period along the [111] direction for fcc metals. This method is limited to this study because our interest is Pb(111) alloy films. In this case, one Pb atom was replaced by a Bi atom in each supercell and the doping content is $1/m^2$, e.g., we use the $\sqrt{7}\times\sqrt{7}\times3$ supercells to describe the $Pb_{0.86}Bi_{0.14}$ alloy films. We found both methods provide almost identical lattice constants in our total-energy calculations. The results are listed in Table I for some concentrations of Bi atoms in Pb. Clearly, the lattice constants of PbBi alloys will become larger than pure Pb.

B. QSE of $Pb_{0.89}Bi_{0.11}$ free-standing alloy films

It can be observed from the phase diagram of the PbBi binary alloy[52] that the alloy will keep the face-centered-cubic structure as the Bi concentration goes up to ~20% at the temperature of 100–200 K. Therefore, we focus on the contents ranging from 5% to 20% for easy comparison with further experimental studies.

We begin with studying the QSE of $Pb_{1-x}Bi_x(111)$ alloy films with $x=0.11$, which has been recently prepared by our group in epitaxial growth.[53] In these alloy films, the ratio of the Pb and Bi atoms is about 8:1. Before studying the QSE of $Pb_{0.89}Bi_{0.11}(111)$ alloy films, it is necessary to discuss the validity of DFT calculation in describing the stability of alloy films by utilizing finite supercells. To this end, we first consider the influence of the distribution of Bi in PbBi alloy films on the stability of films for a given thickness. For the doping content of $x=0.11$, the average distance between the nearest-neighbor bismuth atoms should be about 0.74 nm if we assume that Bi atoms distribute randomly in the bulk Pb. This distance is larger than the third nearest-neighbor distance of Pb atoms. Therefore we conclude that the Bi-Bi interaction in random-alloy films should be weaker.

In our DFT study to simulate film growth of $Pb_{0.89}Bi_{0.11}$ along the direction [111], we adopt the 3×3 supercell in which one of the nine Pb atoms in each layer is replaced by a Bi atom to model the structure of the alloy. Since there is only one Bi atom in each layer, the distance between the two Bi atoms in the base plane is about 1.07 nm. Thus, the interaction between Bi atoms in the base plane should be negligible. Concerning the distance between Bi atoms located at neighboring layers, we consider two extreme cases of Bi distribution. One is that the Bi atoms are well distributed among the Pb atoms and the distance between Bi atoms in neighboring layers is kept as far as possible. In this case, the distance of Bi atoms in two neighboring layers is about 0.62 nm and it is reasonable to assume that the interactions between the Bi atoms are sufficiently weak. Figure 1(a) shows the top view of a five layer $Pb_{0.89}Bi_{0.11}(111)$ alloy film along the. The other case is that the Bi atoms are arranged orderly along the [111] direction and Bi atoms in the neighboring layers are the nearest neighbors, as shown in Fig. 1(b). Obviously, the interaction between Bi atoms in the neighboring layers is strong in this case.

Figures 2(a) and 2(b) show the surface energy from our DFT calculations for the $Pb_{0.89}Bi_{0.11}(111)$ alloy films as a function of the film thickness. The two curves represent two extreme cases in the Bi distribution discussed above. Figure 2(a) represents the second case where the average Bi-Bi distance is maximized, whereas Fig. 2(b) represents the first case where the average Bi-Bi distance is minimized (within the constraint of a 3×3 supercell). We found that the total energy of the latter is always higher than the former for a given thickness. In terms of the surface energy, the latter is

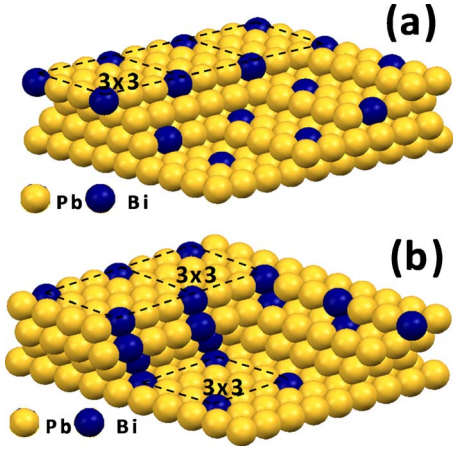

FIG. 1. (Color online) Schematic plot of the structures of $Pb_{0.89}Bi_{0.11}(111)$ alloy film, showing the distribution of Bi atom in Pb. In each layer, one of nine Pb atoms is replaced by one Bi atom. (a) The (111) layers are stacked to maximize the average Bi-Bi distance. (b) The (111) layers are stacked to minimize the average Bi-Bi distance.

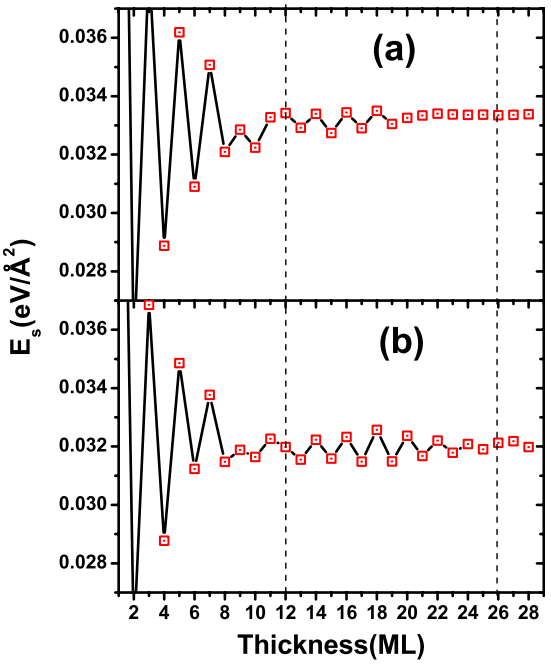

FIG. 2. (Color online) Surface energy of a free-standing $Pb_{0.89}Bi_{0.11}(111)$ alloy slab obtained from DFT calculations. (a) The surface energy of a slab in which Bi atoms are all nearest neighbors in the adjacent (111) layers and (b) the surface energy for maximum Bi-Bi separation.

about 0.034 eV/A^2 while it is 0.032 eV/A^2 for the former at a large thickness. So the configurations with maximum Bi-Bi distance are energetically more stable. It is evident that the surface energy of both types of slabs oscillates with a quasibilayer periodicity, similar to the case of pure Pb(111) films.[30] The Bi distribution seems to have only a marginal effect on the oscillation, although the quantum oscillations are slightly more robust when the average spacing between Bi atoms is maximized. The even-odd crossover in the thin-film stability occurs near 12 ML. Although the use of a 3×3 plane in the supercells for the DFT calculations implies that the Bi atoms are still ordered, it is very unlikely that completely random alloying would produce significantly different results, given the fact that these two cases already represent two extremes in the Bi distribution. So, we believe that the DFT calculations can accurately describe the QSE of alloy films by using a finite supercell size and in the following calculations we only consider the situation that the Bi-Bi distances are maximized.

As shown above, the sequence of the stable films are at 2, 4, 6, 8, 10, 12, 13, 15, 17, 19, 21, 23, 25, 26, 28, and 30 ML while the crossovers are located at 12 ML and 25 ML, respectively. The beating periodicity becomes 13 ML, which is larger than the 9 ML beating periodicity for pure Pb(111) films and this is in agreement with the experimental observations.[53]

We have seen that the film stability depends strongly on the alloy film size as the film surface energy oscillates with the film thickness. It is natural to expect that the work function also depends on the film thickness, deviating from its standard value which is defined for a semi-infinite film. The

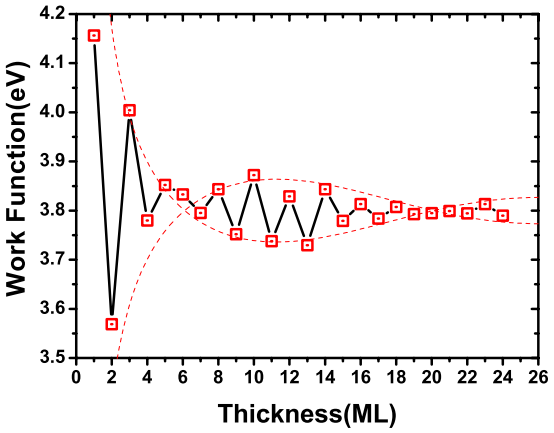

FIG. 3. (Color online) Work function of free-standing $Pb_{0.89}Bi_{0.11}(111)$ alloy film.

results of the work functions of free-standing $Pb_{0.89}Bi_{0.11}(111)$ alloy films as a function of the film thickness are plotted in Fig. 3. From the figure, the first thing to observe is that the work function of the $Pb_{0.89}Bi_{0.11}(111)$ alloy film is found to be about 3.8 eV when the film thickness is more than 25 ML, close to bulk value as expected. This work function is smaller than that of pure Pb(111) films, which is 3.9 eV in our DFT calculations. The decrease in work function can be understood by realizing that the Bi dopants bring additional free electrons to the system. Second, we observe the even-odd oscillations of the work function with the thickness of the films up to 25 ML and the even-odd oscillations are interrupted twice by crossovers owing to the QSE. The crossovers are at the sixth and the 19th layers, so the separation between the crossovers is about 13 ML. Compared with that in the oscillation of surface energy, this beating period in the work-function oscillation is the same but the phases of the beating patterns are different. The location of the crossovers of the work function have a shift of 1/2 beating period compared to the surface energy, lying in the middle of the two crossovers of the surface energy. This discovery is similar to the case of pure Pb films as we have reported in Ref. 30, as well as Pb films on the Si(111) or Cu(111) substrate. Very recently, Miller *et al.*[54] presented an explanation about this effect based on the free-electron model of Pb films and the present work further generalizes its applicability to the PbBi alloy films.

C. Free-standing $Pb_{0.94}Bi_{0.06}$ and $Pb_{0.86}Bi_{0.14}$ alloy films

To investigate the influence of the concentration of the Bi dopants on the quantum size effect, we further calculate the surface energy of the other two free-standing $Pb_{1-x}Bi_x$ alloy films with $x=0.06$ and 0.14 up to 34 ML. We use a 4×4 and a $\sqrt{7}\times\sqrt{7}$ supercell, respectively, and one Pb atom is replaced by one Bi atom in each layer of the supercell. Figures 4(a) and 4(b) show the results of the surface energy and its second derivative of the $Pb_{0.94}Bi_{0.06}$ alloy film as a function of thickness. Similar to the results of the $Pb_{0.89}Bi_{0.11}$ alloy film, the surface energy also demonstrates the bilayer oscillations interrupted by crossovers. However, the separation

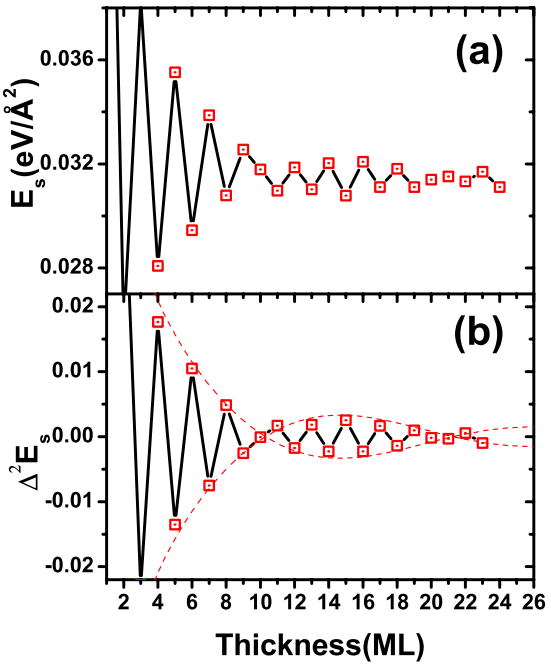

FIG. 4. (Color online) (a) Surface energy of a free-standing $Pb_{0.94}Bi_{0.06}(111)$ alloy film. (b) The discrete second derivative of surface energy of the free-standing $Pb_{0.94}Bi_{0.06}(111)$ alloy film.

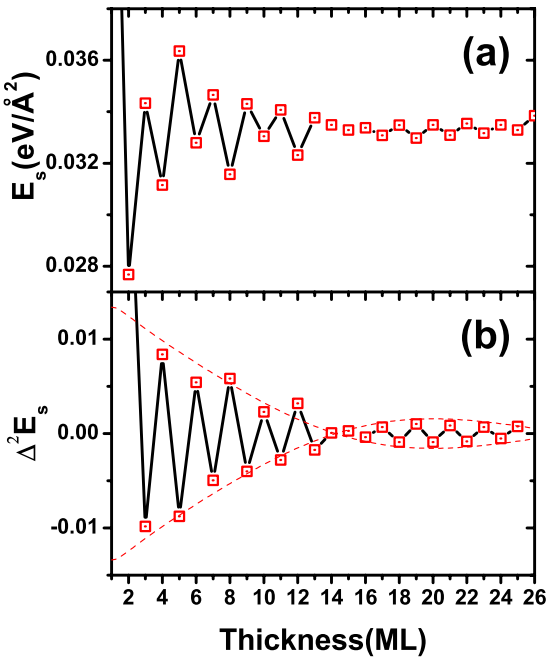

FIG. 5. (Color online) (a) Surface energy of a free-standing $Pb_{0.86}Bi_{0.14}(111)$ alloy film. (b) The discrete second derivative of surface energy of the free-standing $Pb_{0.86}Bi_{0.14}(111)$ alloy film.

between the crossovers is 10 ML and the first crossover locates at the tenth layer, which decreases by 3 ML compared to the case of $Pb_{0.89}Bi_{0.11}$ alloy film. From Fig. 4(b), it can be seen that the films are stable at 2, 4, 6, 8, 10, 11, 13, 15, 17, 19, 21, 22, and 24 ML, and the crossovers are located at 10 and 21 ML.

In Figs. 5(a) and 5(b) we show the results of surface energies and its second derivatives for $Pb_{0.86}Bi_{0.14}$ films. The odd-even oscillation of the surface energy with the film thickness still exists and the magnitude of the oscillation is still relatively large as the film thickness increases up to 20 ML. It is therefore expected that the RBBB growth can be observed experimentally as the doping content increases up to 14%.

For easier comparison, in Table II we list the stability of freestanding $Pb_{1-x}Bi_x$ $(x=0.00, 0.06, 0.11, 0.14)$ alloy films and $Pb_{0.89}Bi_{0.11}$ alloy films on the Si(111) substrate. We use "S" and "U" to denote the stable and unstable films, respectively, and "C" for the position of the crossovers. It is clearly seen in Table II that the stability of the alloy films pursues the bilayer oscillation pattern as the Bi doping content increases up to 14% in the alloy films. However, there are some differences in the details of the patterns between different Bi doping levels. By increasing the content of Bi from 11% to 14%, the beating periodicity shifts from 13 to 16 ML. A simple explanation based on the free-electron theory can be given as follows: As the content of the doping Bi is increased, the Fermi wave vector of the alloy films becomes larger, which leads to a better commensurability between the Fermi wavelength and the interlayer spacing and therefore a larger beating periodicity. Another observation from Table II is the magnitudes of the quantum oscillations become weaker when the content of the Bi dopants is increased. This is consistent with recent experimental observations which show the bilayer-by-bilayer growth mode in the $Pb_{0.8}Bi_{0.2}(111)$ alloy films disappears.[53]

The work function is also influenced by the content of Bi dopants. The results of the $Pb_{0.86}Bi_{0.14}$ alloy films are plotted in Fig. 6. The even-odd oscillations of the work function persist. Given a thickness of the alloy films, the work function is negatively correlated with the Bi dopant content. For example, the work function of the $Pb_{0.86}Bi_{0.14}$ alloy film with the thickness of 25 ML is about 3.70 eV while it is 3.80 eV for the lower doped $Pb_{0.89}Bi_{0.11}(111)$ alloy film with the same thickness. This may be explained by the presence of more free electrons when Bi dopants are increased in lead, which results in an upshifting of the Fermi energy toward the vacuum level and hence reduced work function. The crossover positions of the oscillatory work functions of the two kinds of alloy films, along with that of the free-standing Pb(111) films, are listed in Table III. We see that the positions of the crossovers of the work functions have a phase shift of about half of the beating period comparing with that of the corresponding surface energy.

IV. ROLE OF Si(111) AND Ge(111) SUBSTRATES

To make a better comparison with our recent experiments on the quantum growth of $Pb_{0.89}Bi_{0.11}(111)$ alloy films on Si(111) substrate, it is important to discuss the role of substrates on the QSE of the PbBi(111) alloy films theoretically. As mentioned in Sec. II B, there exists a large mismatch between the lattice constants of the $Pb_{0.89}Bi_{0.11}$ alloy film and the Si(111) or Ge(111) substrates. The large mismatch may result in a stress effect at the interface and bring some artificial errors in the calculated results if we squeeze the lattice

TABLE II. Comparison of the stabilities of $Pb_{1-x}Bi_x$ alloy films both for free standing and on Si(111) substrate, together with the case of pure Pb films. S stands for stable and U for unstable. Crossovers are indicated by C. The wetting layer is included in the table for the films on Si(111) [or Ge(111)] substrate.

		Layer number of $Pb_{1-x}Bi_x$ alloy films																										
Substrate	Content	1	2	3	4	5	6	7	8	9	10	11	12	13	14	15	16	17	18	19	20	21	22	23	24	25	26	
Free standing	$x=0.00$	U	S	U	S	U	S	C	C	S	U	S	U	S	U	S	C	C	S	U	S	U	S	U	S	S		
	$x=0.06$	U	S	U	S	U	S	U	S	U	C	S	U	S	U	S	U	S	U	S	C	U	S	U	S	U		
	$x=0.11$	U	S	U	S	U	S	U	S	U	S	U	C	C	U	S	U	S	U	S	U	S	U	S	U	S		
	$x=0.14$	U	S	U	S	U	S	U	S	U	S	U	S	U	S	C	U	S	U	S	U	S	U	S	U	S	U	
Si(111) or Ge(111) substrate	$x=0.00$ [a]			S	U	C	S	U	S	U	S	U	S	C	U	S	U	S	U	S	U	S	U	C		S		
	Expt.[b] $x=0.00$						S	U	S	U	S	U	S	C	C	S	U	S	U	S	U	S	U	C		S		
	This work $x=0.11$	S	U	S	U	S	C	C	S	U	S	U	S	U	S	U	S	U	S	U	C	C	S	U	S	U	S	
	Expt.[c] $x=0.11$						C	C	S	U	S	U	S	U	S	U	S	U	S	U	C	C	S	U	S	U	S	

[a]Reference 26.
[b]References 13 and 26.
[c]Reference 52.

of substrate to match that of the $Pb_{0.89}Bi_{0.11}$ alloy films. To overcome this problem, we use a Si(111)-$\sqrt{7}\times\sqrt{7}$ surface unit cell to match the $Pb_{0.89}Bi_{0.11}$(111)-3×3 unit cell by rotating the substrate by 19.1°, leading to a almost perfect lattice match at the interface, shown in Fig. 7. However it still results in a mismatch of the lattice constants of about 3% at the interface. Before the recent studies of quantum growth of ultrathin metal films, people generally thought that the effects of stress is the most important factor in heteroepitaxial growth. While this is true for semiconductors and insulators, the electronic driving force can be much stronger than the strain effects in dictating the growth modes in the ultrathin film regime.[55] Lead is known to be a soft metal and the strain energy built up in the film as the film thickness increases is therefore much weaker than the electronic effects and can be ignored. For this reason, we have chosen to expand the Si substrate by ~3% after the rotation for perfect lattice matching. This choice introduces a finite but constant strain energy term associated with the substrate but no related strain energy buildup in the metal films. Therefore, the constant strain energy term does not affect the conclusions and predictions of our theoretical study, as reflected by the excellent agreement with the experimental observations. We also note that, as pointed out in our earlier study,[30] such a small degree of lattice expansion does not alter the fundamental semiconductor nature of Si.

In calculations, we obtained almost the same results for $Pb_{0.89}Bi_{0.11}$(111) alloy films on Si(111) or Ge(111) substrates. Figures 8(a) and 8(b) show the surface energy and its second derivative of the $Pb_{0.89}Bi_{0.11}$(111) alloy films on the Si(111) substrate. Similar to the free-standing $Pb_{0.89}Bi_{0.11}$ alloy films discussed above, there are also bilayer oscillations interrupted by crossovers in this system. The separation between the crossovers is the same as the free-standing alloy film but the positions of the crossovers are located at the seventh and the 20th MLs, respectively, which are different from the case of the free-standing alloy film. We find that the stable films are 3, 5, 7, 8, 10, 12, 14, 16, 18, 20, 21, 23, and 25 ML from Fig. 8(b). These results agree almost perfectly with a recent experiment of the $Pb_{0.89}Bi_{0.11}$(111) alloy films on the Si(111) substrate.[53] (In the experimental results, the 1-ML-thick wetting layer is excluded from the thickness counting, see Ref. 26). This indicates that our first-principles calculations have successfully described the essential physics of $Pb_{0.89}Bi_{0.11}$ alloy films growth on the Si(111) substrate.

Finally, the crossover positions and the separation of the crossovers are different due to the different concentrations of the dopant and the substrates as well. We also list the crossover positions for both the surface energy and work function of $Pb_{0.89}Bi_{0.11}$ alloy films on the Si(111) substrate in Table II.

V. FREE-ELECTRON MODEL

For pure Pb(111) films, the free-electron model has been used to understand the QSE in their growth behaviors.[27,29] According to the free-electron model, the bilayer oscillations are the results of the ratio $k_F:k_{BZ}\approx4:3$ ($k_{BZ}=\pi/d_0$) in the Pb (111) films, where d_0 is the lattice plane spacing along the [111] direction. However, its equivalence to 4/3 is only approximate and a small deviation from the exact 4:3 ratio will

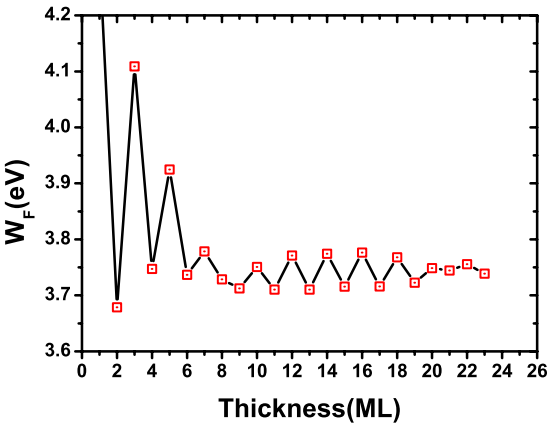

FIG. 6. (Color online) Work function of the free-standing $Pb_{0.86}Bi_{0.14}$ alloy film.

TABLE III. Crossover positions of $Pb_{1-x}Bi_x(111)$ alloy films for three different concentrations.

	Pb free standing[a] $x=0.00$			$x=0.06$			$x=0.11$			$x=0.14$		
	First	Second	Third	First	Second	Third	First	Second	Third	First	Second	Third
$\mathbf{E_S}$	8	17	26	10	20		12	25		15		
$\mathbf{W_F}$	4	13	22	5	15	25	6	19		8	24	

[a]Reference 30.

accumulate as the film grows thicker, leading to the appearance of crossovers. The beating period of the crossovers is then given by

$$\lambda_{beat} = \frac{\pi}{3k_{BZ} - 2k_F}. \tag{3}$$

By using the experimental value of k_{BZ} (1.59 $Å^{-1}$) and d_0 (2.84 Å) in Pb(111), we can obtain the beating period of the crossovers from Eq. (3), which is 9.3 ML.

Can we at least understand the above DFT results qualitatively with this free-electron model? Since the lattice constant of PbBi alloy does not change much as one varies the concentration of the Bi atoms from our calculations, the change in the beating period should be mainly caused by the change in k_F due to the metal dopants. In the free-electron model, the Fermi wave vector is given by[56]

$$k_F = (3\pi^2 n)^{1/3}, \tag{4}$$

where n is the electron density. In $Pb_{1-x}Bi_x(111)$ alloy films, the free-electron density is approximately given by the formula

$$n_{Pb_{1-x}Bi_x} = (1-x)n_{Pb} + xn_{Bi}. \tag{5}$$

Since bismuth has five valence electrons and lead has four, we take $n_{Bi}=5/4n_{Pb}$ approximately. From Eqs. (3)–(5), we can obtain the beating period of $Pb_{1-x}Bi_x$ alloy film for different contents of Bi. For example, for $x=0.11$, the electron density will be increased by 2.75% compared to the pure Pb films. This in turn increases the Fermi wave vector by 0.9% and the associated beating period should increase from 9.3 to 12.7 ML, calculated by Eq. (3). This is in excellent agreement with both the experimental and our DFT results, namely, 13 ML.

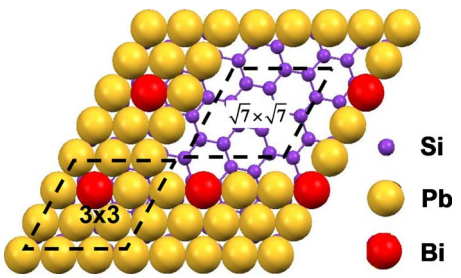

FIG. 7. (Color online) Top view of interface structure of $Pb_{0.89}Bi_{0.11}(111)$ alloy films on Si(111). It shows the match between a $\sqrt{7}\times\sqrt{7}$ unit cell of Si (111) and a 3×3 unit cell of $Pb_{0.89}Bi_{0.11}(111)$ films.

The beating periods for various contents of Bi calculated using the free-electron model, together with the DFT results, are plotted in Fig. 9. In the cases of low doping content, we can find from Fig. 9 that the free-electron model is in good agreement with DFT results.

When the doping level increases, the results of the free-electron model deviate from the DFT results. This can be understood by the fact that there will be more scattering centers with more dopants in the lead films. To show this point clearly, we have also calculated the charge distributions around the Bi atoms in Pb(111) films by using a $3\times3\times12$ supercell. The calculation was done by the following formula:

$$\Delta\rho(z) = \int\int \rho_{PbBi}(x,y,z)dxdy - \int\int \rho_{Pb}(x,y,z)dxdy, \tag{6}$$

where x, y, and z are the coordinate of the supercell. Two cases are considered in the calculations. One is that only one Pb atom is replaced by Bi atom in the supercell and the other in each monolayer. The results are shown in Figs. 10(a) and 10(b), respectively. From Figs. 10(a) and 10(b), we can see that the extra charge prefers to be delocalized around Bi atoms at a given doping level. However, as the doping level increases, more and more scattering centers are introduced in

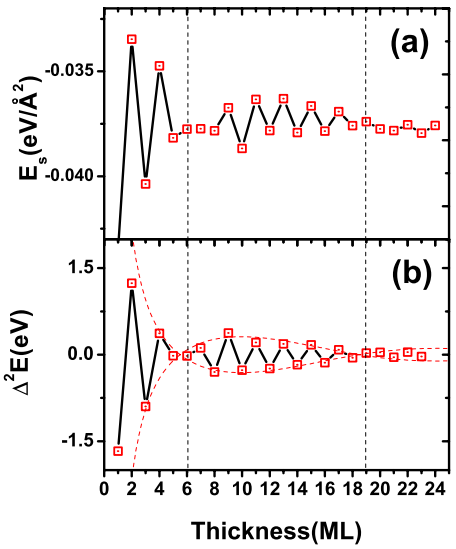

FIG. 8. (Color online) (a) Surface energy of a $Pb_{0.89}Bi_{0.11}$ alloy film on Si(111) substrate and (b) the discrete second derivative of surface energy of the $Pb_{0.75}Bi_{0.25}$ alloy film on Si(111).

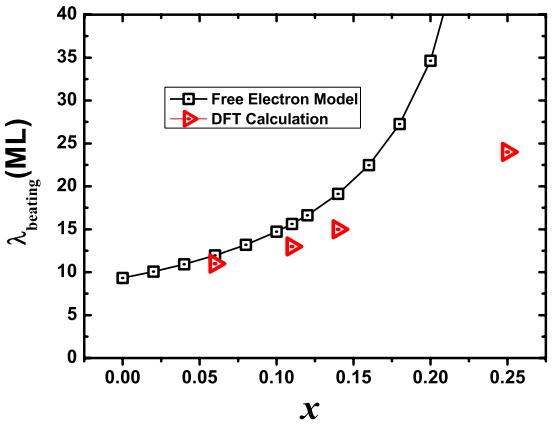

FIG. 9. (Color online) The beating periods for vary contents of Bi calculated in the free-electron model and the first-principle calculations.

the PbBi films, resulting in invalidation of the free-electron model.

VI. SUMMARY AND DISCUSSIONS

Using density-functional theory calculations, we have studied the effect of doping Bi in Pb(111) ultrathin films on tuning the quantum size effects of the ultrathin random-alloy films. The influences of different doping levels and substrates have also been explored. Our results demonstrate that the QSE of the Pb(111) film is very robust against the introduction of random dopants inside the film. Specifically, the stability of ultrathin $Pb_{1-x}Bi_x(111)$ random-alloy films exhibits strong quantum oscillations up to 20% Bi dopant concentration and the spatial distribution of the dopants only has a marginal effect on the thin-film stability. Our theoretical results also show that the periodicity and phase shift of the beating patterns of the oscillations are determined by the Fermi wave vector, which can be tuned via the dopant concentration and the substrate as well. The calculated crossover

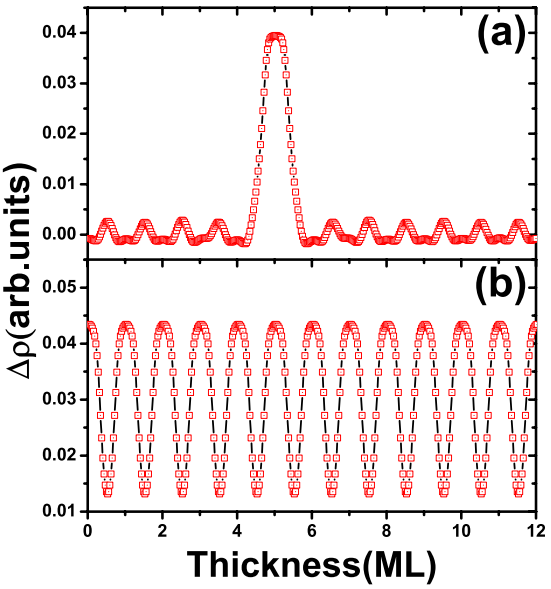

FIG. 10. (Color online) Charge distribution of Bi atoms as dopants in Pb(111) films, (a) one isolated Bi atom and (b) one Bi atom in each Pb layer.

positions and the beating periodicity of the stability of the $Pb_{0.89}Bi_{0.11}$ alloy films are in good agreement with our recent experimental observations.

ACKNOWLEDGMENTS

We thank Yuping Huo for helpful discussions, and Brandon Bell and Hua Chen for critical readings of the manuscript. Y.J. and S.Y.W. is supported by NSF of China (Grants No. 10974182 and No. 10974029). H.H.W. and Z.Z. are supported by the U.S. NSF (Grant No. DMR-0906025) and in part by the Division of Materials Science and Engineering, Basic Energy Sciences, U.S. DOE. The calculations were performed at DOE's NERSC and Center for Computational Sciences of Zhengzhou University, China.

[1] Z. Y. Zhang, Surf. Sci. **571**, 1 (2004).
[2] A. R. Smith, K.-J. Chao, Q. Niu, and C.-K. Shih, Science **273**, 226 (1996).
[3] Y. Qi, X. Ma, P. Jiang, S. Ji, Y. Fu, J.-F. Jia, Q.-K. Xue, and S. B. Zhang, Appl. Phys. Lett. **90**, 013109 (2007).
[4] Y.-F. Zhang, Z. Tang, T.-Z. Han, X.-C. Ma, J.-F. Jia, Q.-K. Xue, K. Xun, and S.-C. Wu, Appl. Phys. Lett. **90**, 093120 (2007).
[5] X. Ma, P. Jiang, Y. Qi, J. Jia, Y. Yang, W. Duan, W.-X. Li, X. Bao, S. B. Zhang, and Q.-K. Xue, Proc. Natl. Acad. Sci. U.S.A. **104**, 9204 (2007).
[6] P. Jiang, X. Ma, Y. Ning, C. Song, X. Chen, J.-F. Jia, and Q.-K. Xue, J. Am. Chem. Soc. **130**, 7790 (2008).
[7] Y. Guo, Y.-F. Zhang, X.-Y. Bao, T.-Z. Han, Z. Tang, L.-X. Zhang, W.-G. Zhu, E. Wang, Q. Niu, Z. Qiu, J.-F. Jia, Z.-X. Zhao, and Q.-K. Xue, Science **306**, 1915 (2004).
[8] M. M. Özer, J. R. Thompson, and H. H. Weitering, Nat. Phys. **2**, 173 (2006).
[9] Y.-F. Zhang, J.-F. Jia, T.-Z. Han, Z. Tang, Q.-T. Shen, Y. Guo, Z. Q. Qiu, and Q.-K. Xue, Phys. Rev. Lett. **95**, 096802 (2005).
[10] F. Yndurain and M. P. Jigato, Phys. Rev. Lett. **100**, 205501 (2008).
[11] L. Gavioli, K. R. Kimberlin, M. C. Tringides, J. F. Wendelken, and Z. Y. Zhang, Phys. Rev. Lett. **82**, 129 (1999).
[12] D.-A. Luh, T. Miller, J. J. Paggel, M. Y. Chou, and T.-C. Chiang, Science **292**, 1131 (2001).
[13] K. Budde, E. Abram, V. Yeh, and M. C. Tringides, Phys. Rev. B **61**, R10602 (2000).
[14] M. Hupalo, V. Yeh, L. Berbil-Bautista, S. Kremmer, E. Abram, and M. C. Tringides, Phys. Rev. B **64**, 155307 (2001).
[15] M. Hupalo, S. Kremmer, V. Yeh, L. Berbil-Bautista, E. Abram, and M. C. Tringides, Surf. Sci. **493**, 526 (2001).
[16] W. B. Su, S. H. Chang, W. B. Jian, C. S. Chang, L. J. Chen, and

T. T. Tsong, Phys. Rev. Lett. **86**, 5116 (2001).
[17] S. H. Chang, W. B. Su, W. B. Jian, C. S. Chang, L. J. Chen, and T. T. Tsong, Phys. Rev. B **65**, 245401 (2002).
[18] H. Okamoto, D. Chen, and T. Yamada, Phys. Rev. Lett. **89**, 256101 (2002).
[19] H. Hong, C.-M. Wei, M. Y. Chou, Z. Wu, L. Basile, H. Chen, M. Holt, and T.-C. Chiang, Phys. Rev. Lett. **90**, 076104 (2003).
[20] W. B. Su, S. H. Chang, H. Y. Lin, Y. P. Chiu, T. Y. Fu, C. S. Chang, and T. T. Tsong, Phys. Rev. B **68**, 033405 (2003).
[21] J. H. Dil, J. W. Kim, S. Gokhale, M. Tallarida, and K. Horn, Phys. Rev. B **70**, 045405 (2004).
[22] C.-S. Jiang, S.-C. Li, H.-B. Yu, D. Eom, X.-D. Wang, P. Ebert, J.-F. Jia, Q.-K. Xue, and C.-K. Shih, Phys. Rev. Lett. **92**, 106104 (2004).
[23] X.-Y. Bao, Y.-F. Zhang, Y. Wang, J.-F. Jia, Q.-K. Xue, X. C. Xie, and Z.-X. Zhao, Phys. Rev. Lett. **95**, 247005 (2005).
[24] R. Otero, A. L. Vazquez de Parga, and R. Miranda, Phys. Rev. B **66**, 115401 (2002).
[25] A. Crottini, D. Cvetko, L. Floreano, R. Gotter, A. Morgante, and F. Tommasini, Phys. Rev. Lett. **79**, 1527 (1997).
[26] M. M. Özer, Y. Jia, B. Wu, Z. Y. Zhang, and H. H. Weitering, Phys. Rev. B **72**, 113409 (2005).
[27] Z. Zhang, Q. Niu, and C.-K. Shih, Phys. Rev. Lett. **80**, 5381 (1998).
[28] F. K. Schulte, Surf. Sci. **55**, 427 (1976).
[29] B. Wu and Z. Zhang, Phys. Rev. B **77**, 035410 (2008).
[30] Y. Jia, B. Wu, H. H. Wertering, and Z. Zhang, Phys. Rev. B **74**, 035433 (2006).
[31] T.-C. Chiang, Surf. Sci. **39**, 181 (2000).
[32] G. Palasantzas and J. T. M. De Hosson, Phys. Rev. B **63**, 125404 (2001).
[33] Z. Q. Qiu and N. V. Smith, J. Phys.: Condens. Matter **14**, R169 (2002).
[34] A. E. Meyerovich and I. V. Ponomarev, Phys. Rev. B **67**, 165411 (2003).
[35] B. J. Hinch, C. Koziol, J. P. Toennies, and G. Zhang, Europhys. Lett. **10**, 341 (1989).
[36] J. Braun and J. Toennies, Surf. Sci. **384**, L858 (1997).
[37] P. Czoschke, H. Hong, L. Basile, and T.-C. Chiang, Phys. Rev. Lett. **91**, 226801 (2003).
[38] L. Floreano, D. Cvetko, F. Bruno, G. Bavdek, A. Cossaro, R. Gotter, A. Verdini, and A. Morgante, Prog. Surf. Sci. **72**, 135 (2003).
[39] C. M. Wei and M. Y. Chou, Phys. Rev. B **66**, 233408 (2002).
[40] P. Hohenberg and W. Kohn, Phys. Rev. **136**, B864 (1964).
[41] W. Kohn and L. Sham, Phys. Rev. **140**, A1133 (1965).
[42] G. Kresse and J. Hafner, Phys. Rev. B **47**, 558 (1993).
[43] G. Kresse and J. Furthmüller, Comput. Mater. Sci. **6**, 15 (1996).
[44] G. Kresse and J. Furthmüller, Phys. Rev. B **54**, 11169 (1996).
[45] J. P. Perdew and Y. Wang, Phys. Rev. B **45**, 13244 (1992).
[46] D. Vanderbilt, Phys. Rev. B **41**, 7892 (1990).
[47] H. J. Monkhorst and J. D. Pack, Phys. Rev. B **13**, 5188 (1976).
[48] M. Methfessel and A. T. Paxton, Phys. Rev. B **40**, 3616 (1989).
[49] J. C. Boettger, Phys. Rev. B **53**, 13133 (1996).
[50] J. C. Boettger, Phys. Rev. B **49**, 16798 (1994).
[51] J. G. Gay, J. R. Smith, R. Richter, F. J. Arlinghaus, and R. H. Wagoner, J. Vac. Sci. Technol. A **2**, 931 (1984).
[52] R. Hultgren, P. D. Desai, D. T. Hawkins, M. Gleiser, and K. K. Kelley, *Selected Values of the Thermodynamic Properties of Binary Alloy* (American Society for Metals, Metals Park, OH, 1973).
[53] M. M. Ozer, Y. Jia, Z. Zhang, J. R. Thompson, and H. H. Wertering, Science **316**, 1594 (2007).
[54] T. Miller, M. Y. Chou, and T. C. Chiang, Phys. Rev. Lett. **102**, 236803 (2009).
[55] Z. G. Suo and Z. Y. Zhang, Phys. Rev. B **58**, 5116 (1998).
[56] N. W. Ashcroft and N. D. Mermin, *Solid State Physics* (Holt, Rinehart and Winston, New York, 1976).